

# BREAKING IMAGING LIMITS USING DITHERING MASKS IN 0.35 TERAHERTZ SINGLE-PIXEL IMAGING

*S. Augustin*<sup>1,2</sup>, *T. Szollmann*<sup>3</sup>, *P. Jung*<sup>3</sup>, *H.-W. Hübers*<sup>1,2</sup>

<sup>1</sup>Humboldt Universität zu Berlin, Department of Physics, 10099 Berlin, Germany.

<sup>2</sup>German Aerospace Center (DLR), Institute of Optical Sensor Systems, 12489 Berlin, Germany.

<sup>3</sup>Technische Universität Berlin, Department of Electrical Engineering and Computer Science, 10587 Berlin, Germany.

## ABSTRACT

In this contribution, we explore the imaging limits of terahertz single-pixel cameras and present a way to improve the achievable signal-to-noise ratio and spatial resolution using a technique called *dithering masks*. The proposed procedure is implemented on the hardware level using recent advances in the development of spatial light modulators for terahertz single-pixel cameras. Thereby, our approach offers new ways to overcome theoretical imaging limits of near wavelength resolution. We suggest that in using dithering masks the required phase retrieval driven recovery can be simplified to a robust non-negative linear model even for near wavelength terahertz single-pixel imaging.

**Index Terms**— single-pixel camera, 0.35 terahertz, dithering masks, non-linear effects, increased spatial resolution, phase retrieval

## 1. MOTIVATION & INTRODUCTION

Single-pixel cameras (SPCs) [1] have found widespread use in many areas both on the research level and also in the industrial domain. In particular, SPCs that work outside of the visible have quickened interests in many fields. The advantages of the single-pixel approach, which are the possibility for signal processing on the hardware level (computational imaging) and the image acquisition with a stationary single detector pixel, are especially beneficial in fields where a single detector pixel is multiple times more expensive than a detector pixel in the VIS domain or where multiple pixel cameras are not readily available (due to various physical reasons). This is exactly true for the low terahertz (THz) domain and in particular for 0.35 THz.

0.35 THz radiation is of special interest because it is electromagnetic radiation with a somewhat unique combination of advantageous properties. It is able to penetrate many optical obstructions like packaging material, clothing, insulation material, etc. This property is, of course, similar to

*X-ray*'s. But on the other hand *X-ray*'s are so-called ionizing radiation, which can damage living cells and in general are harmful to organic tissue. In contrast terahertz is non-ionizing radiation, which is harmless for living cells and also for organic tissue in general. Additionally, terahertz has the advantageous property to sufficiently interact with the material it penetrates, retaining the ability to make objects visible that cannot be visualized with other means. Applications that would make use of this unique combination of advantageous properties are for example a terahertz camera that is able to visualize the processes inside living cells or the behavior of electrons inside quantum electronic devices.

**Prior Work on THz single-pixel imaging:** One of the first publications on the idea of THz single-pixel imaging is reported in [2]. Here, the spatially-structured masks were implemented as metallic filters that had to be changed by hand, due to the lack of suitable THz spatial light modulators (SLMs). One of the first non-manual implementations is published in [3]. Subsequent publications by various groups adapted the single-pixel THz idea to improved setups with differing THz sources and also differing implementations of the THz-SLM [4–7]. In recent years a group in England reported the application of the single-pixel idea for near field imaging with spatial resolution well-below the wavelength [8]. However, far field single-pixel THz imaging with well-below wavelength resolution has not been reported so far.

**Main Contribution:** We establish the connection between single-pixel 0.35 THz imaging and diffraction. The influence of diffraction prohibits the usual linear intensity model and leads therefore to a non-linear imaging model that is similar to the well-known phase-retrieval problem. Since such problems are numerically challenging it is necessary, for real-time camera operation, to have appropriate linear approximations. In this work we, therefore, propose the application of dithering masks. Commanding these masks to the SLM allows for a robust, linearized imaging operation of single-pixel THz cameras. Under these conditions recovery is achieved using an efficient, non-negative least squares approach (NNLS).

Thanks to the German Research Foundation (DFG) for funding the work presented here in the scope of the priority program SPP1798 Compressed Sensing in Information Processing (CoSIP) grants HU848/7 and JU2795/3.

The imaging modality for a 0.35 THz SPC that is of interest here is the use of the camera in a far-field imaging modality, where the scene is several centimeters away from the camera. This modality is especially appealing for the given envisioned application examples. To get an idea of the complexity and the distances involved, Fig. (1) shows at the left-hand side a block diagram and in the right-hand side a representation of the 0.35 THz SPC used for the experiments discussed here.

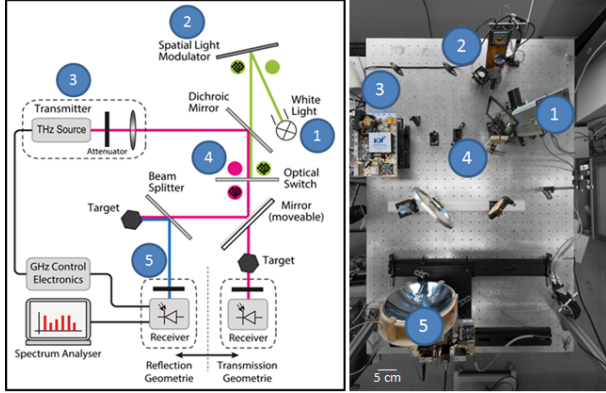


**Fig. 1.** Representation of the 0.35 terahertz single-pixel camera used for the experiments discussed here.

In this text we will explore the hardware signal processing ability and overall operation of a 0.35 THz SPC. To overcome the identified limitations a method based on dithering masks is presented, which will pave the way towards enabling the unique applications mentioned above. The text is thereby structured as follows. The next section introduces the terahertz single-pixel camera approach by discussing an imaging example and the respective measurement signals for standard 0.35 THz SPC operation. Section (3) then derives the limits of standard camera operation and supports them by both experimental and theoretical findings. Finally, the novel dither method is introduced.

## 2. STANDARD 0.35 TERAHERTZ SINGLE-PIXEL CAMERA OPERATION

A single-pixel camera is able to image a scene of interest with just a single detector pixel because the multiple acquisitions that are carried-out in parallel in a multi-pixel camera are carried-out sequentially in a single-pixel camera. The ability to substitute parallel image acquisition for sequential acquisition is possible due to the use of a spatial light modulator (SLM). The SLM is used to project patterns (masks) onto a scene of interest and the response from this projection is measured by the single detector pixel. The necessary number of sequential acquisitions depends (i) on the compressibility

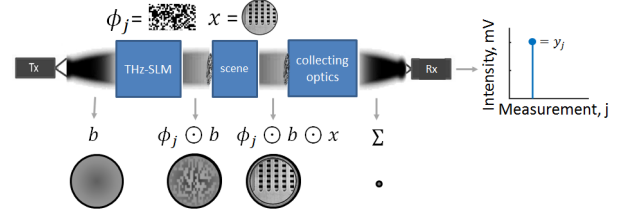


**Fig. 2.** Visualization of the single-pixel camera measurement process according to the linear imaging model of (1).

of the scene itself (like sparsity in a known basis) (ii) the properties of the masks and (iii) the method used for image reconstruction. The interconnection of the aforementioned aspects is non-linear and directly influences the performance of the imaging process in terms of spatial resolution, imaging speed, image quality, etc. Accordingly, the full model which is used to describe the imaging process is also non-linear. However, on a generic level, the standard operation of a 0.35 THz SPC can be described using a linearized imaging model as in (1) and visualized in Fig. (2).

$$y = A \cdot x + n \quad (1)$$

In (1),  $y$  denotes the vector of measured values,  $A$  is the measurement matrix, which contains in each row the effective masks used for the imaging process and  $n$  models an additive noise component.  $x$  is the (vectorized) object in the scene to be reconstructed from the measurements. A typical assumption in compressed sensing is that  $x = \Psi\alpha$  where  $\Psi$  is a known sparsifying transformation and  $\alpha$  is a vector of transform coefficients that essentially concentrates only on few but unknown coordinates ( $\alpha$  is sparse).

In this context, the inverse problem (1) is meanwhile well-understood and, if possible, certain random matrices achieve optimal performance in terms of sampling rate and reconstruction accuracy. On the other hand, one of the main challenges in practical experiments is the optimization of the overall measurement setup in a way to come close to such a model. Often the linear model has (i) to be modified to account for other effects, like non-uniform illumination and (ii) is valid only in a sense of a certain approximation since, the detector may behave non-linearly and the other optical components have relevant influence. Finally, (iii) diffraction will play a role.

In our case, we have to, additionally, account for the beam profile  $b$ , SLM effects and the detector measuring only integrated intensities. As measurement masks pseudo-random binary masks  $\{\phi_j\}$  are commanded to the SLM and chosen here also due to their empirical robustness properties with respect to such model uncertainties (and their incoherence to a wide variety of transformations). Except of the effects due to (ii) and (iii), the imaging process is further illustrated in Fig. (2). The beam  $b$  from the terahertz source (Tx) is spatially

modulated by the  $j$ th mask  $\phi_j$  commanded to the single-pixel cameras SLM. The spatially modulated beam  $\phi_j \odot b$  is then used to probe the scene  $x$  and the entire response  $\phi_j \odot b \odot x$  from the scene is integrated into a single-measurement value  $\langle \phi_j \odot b, x \rangle$  of the camera's single detector pixel. In short, every commanded mask leads to one measurement value. To image the entire scene a number of masks commensurate to the information content in the scene and the desired spatial resolution has to be measured. Following the imaging model (1) an example measurement is shown in Fig. (3).

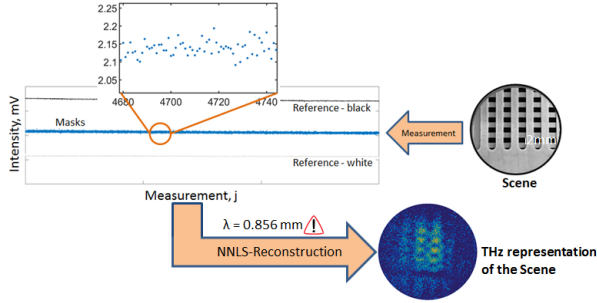


**Fig. 3.** Example measurement and reconstruction of the measured values using the 0.35 THz SPC in standard measurement mode. As reconstruction algorithm non-negative least squares was used. Note, that the terahertz representation of the scene is inverted in regard to the photograph.

On the left-hand side of the figure the measured mask characteristic is shown. The characteristic is comprised of three lines which show more or less variation depending on the respective commanded mask, model error and additive measurement noise. The top line shows the measurement response of commanded, spatially unstructured black masks. The lowest line results from commanded, spatially unstructured white masks. The middle line, which shows the largest variation, results from the spatially structured masks. Only this line carries spatial information about the scene. The information from the other two lines is simply used to adapt the terahertz camera to changing measurement conditions (measurement overhead). The information encoded in the variation of the middle line is used to reconstruct a terahertz representation of the measured scene. The reconstruction is shown in the bottom part of Fig. (3).

The reconstruction shows that the periodic structure of the scene object was captured with a spatial resolution better than the wavelength. However, as is visible the spatial resolution is changing over the field-of-view of the camera and the reconstruction quality itself is also not homogeneous. The edges of some of the features in the image are not straight and are smeared out over several pixels. These artifacts are partially caused by deviations from the initial linear model (1). In the next section we will, therefore, present an imaging method which accounts for diffraction effects and still comes with the advantage of a linear imaging model. Starting from a full non-

linear imaging model that is related to the well-known phase-retrieval problem we will establish a modified description that is applicable to single-pixel imaging with dithering masks.

### 3. IMAGING LIMITS OF STANDARD 0.35 TERAHERTZ SINGLE-PIXEL CAMERAS

As introduced in the last section, it is hypothesized that the limits of standard single-pixel camera operation stem from an inadequate imaging model. The linearized model Eqn. (1) is working adequately when the structures (block size) in the commanded masks are multiple times larger than the wavelength (0.35 THz  $\equiv$  0.85 mm). On the other hand the size of the mask structures are directly responsible for the spatial resolution that is achievable with a single-pixel camera. It means that the standard operation of a 0.35 THz SPCs is limited to spatial resolution at the order of the wavelength. The cause of this limitation can be derived from the imaging model when the full imaging model is analyzed. In the following we will sketch particular steps towards a linear model and discuss some difficulties, which can arise for a practical device.

The starting point is the well-known diffraction integral [9]. For brevity of exposition we use generic two-dimensional coordinates  $(u, v)$  without discretization. Assume that the detector position is at  $z = 0$  on the optical axis and denote with  $\mathcal{T}$  the target surface at position  $z = d_{\mathcal{T}}$ . Then, the  $j$ th measurement of the target  $x = x(u, v)$  with an effective mask  $\phi_j^{\text{THz}} = \phi_j^{\text{THz}}(u, v)$  – which may differ from commanded masks  $\phi_j$  – given (up to additive noise) as the magnitude of the following diffraction integral<sup>1</sup>.

$$y_j \sim \left| \iint_{\mathcal{T}} \phi_j^{\text{THz}} \cdot x \frac{e^{ikr}}{r} dudv \right|, \quad (2)$$

with  $r = \sqrt{u^2 + v^2 + d_{\mathcal{T}}^2}$  and wave number  $k$ . With the far field assumption (by using a lens), we assume that up to further scaling factors, the measurements can be written as:

$$y_j \sim \left| \iint_{\mathcal{T}} \phi_j^{\text{THz}} \cdot x dudv \right|, \quad (3)$$

However, the effective masks  $\phi_j^{\text{THz}}$  are obtained by transferring the commanded, binary masks  $\phi_j$  from the mask surface  $\mathcal{M}$  at  $z = d_{\mathcal{M}}$  to target scene  $\mathcal{T}$  via a diffraction integral operator:

$$\phi_j^{\text{THz}}(u', v') \sim \iint_{\mathcal{M}} (\phi_j b + (1 - \phi_j) a) \frac{e^{ikr'}}{r'} dudv \quad (4)$$

with  $r' = \sqrt{(u' - u)^2 + (v' - v)^2 + (d_{\mathcal{M}} - d_{\mathcal{T}})^2}$ . Recall that  $b = b(u, v) \geq a(u, v) = a \geq 0$  are the beam profile and SLM offset. Obviously, (4) is related to the Fourier transform

<sup>1</sup>We use  $a \sim b$  to indicate that, up to constants,  $a$  is equal to  $b$  (approximation).

for  $d_{\mathcal{M}} - d_{\mathcal{T}} \rightarrow \infty$ . Thus, an important design criterion is to command masks with sufficiently large block size such that for small  $z$  the operation above is close to the identity (See Fig. (4) for a simulation of one mask with varying block size as evidence for this statement.)

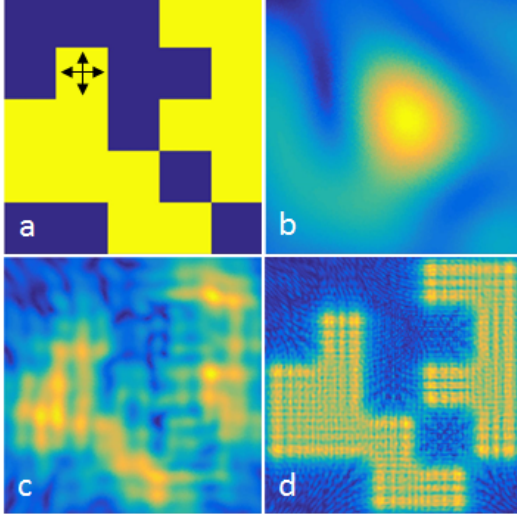


**Fig. 4.** Simulation showing the distortions between the commanded masks (a) and the imaging masks for the 0.35 terahertz single-pixel camera considering mask block sizes of 1 mm (b), 3 mm (c) and 10 mm (d). The arrows indicate a random mask block. All images b-d also show some under-sampling artifacts of the simulation.

Then (2) is approximately (up to constants and additive noise):

$$y_j \approx \iint_{\mathcal{T}} (\phi_j b + (1 - \phi_j) a) \cdot x \, dudv \quad (5)$$

In practice the imaging device needs to be calibrated as well but this subject is still an open research topic. After suitable discretization and for given non-negative  $a$  and  $b$ , the problem can be described again with a measurement matrix  $A$  as (1). Due to non-negativity and additional properties of  $A$  (see here the  $\mathcal{M}^+$ -criterion in [10]) the target can be reconstructed using a non-negative least-squares (NNLS) approach:

$$\min_{x \geq 0} \|Ax - y\|_{\ell_2} \quad (6)$$

This problem can be solved using, for example, active set algorithms. Meanwhile also other very efficient methods are available, see e.g. [11]. In particular, our results are obtained using FLEXBOX [12]. Note that, due to the non-negativity this approach still allows for subsampling and is related to  $\ell_1$ -self-regularization, see [13]. Indeed, for random iid. binary matrices even optimal subsampling can be achieved for sparse  $x$  [10] and similar conclusion can be drawn for certain other

sparsity domains  $\Psi$ .

Obviously, the full nonlinear diffraction model would describe the interdependence between the measurement values  $y$  and the wavelength  $\lambda$  of the radiation used in the single-pixel camera. But the current state-of-the-art approaches in phase retrieval still require numerically challenging algorithms and guarantees for randomized but practically relevant measurement models are rare. So far, there are no accurate algorithms which can solve (2) in a quasi real-time fashion. Therefore the question arises, whether it is possible to still work with a sufficiently accurate linearized model (1) and at the same time, produce spatial resolution better than the size of the wavelength.

**Dithering Masks explained:** To overcome the wavelength limitations in THz single-pixel imaging we propose the use of dithering masks for improved single-pixel camera operation. Dithering masks thereby means the use of masks with a large block size. These blocks are then shifted by random offsets in the order of the wavelength. Such a mask set should theoretically provide a large signal-to-noise ratio while keeping the high-resolution capabilities of a single-pixel setup. Additionally, such a mask set should not suffer from the mask degradation effects introduced above. The construction of a dithering masks set as well as a reconstruction using such a mask set are illustrated in Fig. (5).

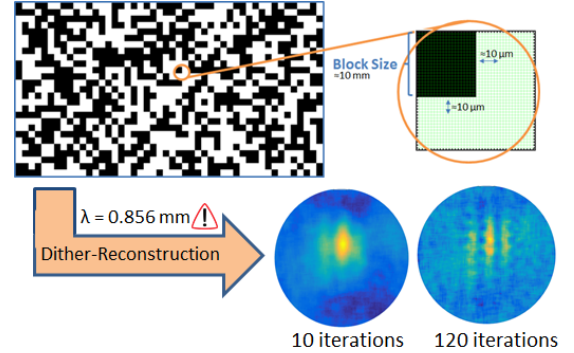


**Fig. 5.** Illustration of the construction of a dithering mask set and a reconstruction using such a set (visualization of shifts not up to scale).

As can be seen the reconstruction with the dither mask set shows more homogeneous reconstruction results than the standard reconstruction of Fig. (3). The edges of the reconstructed features are straight and not smeared out over several pixels, indicating a better spatial resolution. However it is noteworthy that the reconstruction success crucially depends on the chosen reconstruction parameter combination and the number of iterations of the reconstruction algorithm.

**Acknowledgements:** The authors are very grateful to Hendrik Dirks for his support with the software reconstruction of the presented data using [12].

#### 4. REFERENCES

- [1] Marco F. Duarte, Mark A. Davenport, Dharmpal Takhar, Jason N. Laska, Ting Sun, Kevin F. Kelly, and Richard G. Baraniuk, "Single-pixel imaging via compressive sampling," *IEEE Signal Processing Magazine*, vol. 25, no. 2, pp. 83–91, 2008.
- [2] Wai Lam Chan, Kriti Charan, Dharmpal Takhar, Kevin F. Kelly, Richard G. Baraniuk, and Daniel M. Mittleman, "A single-pixel terahertz imaging system based on compressed sensing," *Applied Physics Letters*, vol. 93, no. 12, pp. 121105, 2008.
- [3] Stefan Busch, Benedikt Scherger, Maik Scheller, and Martin Koch, "Optically controlled terahertz beam steering and imaging," *Optics letters*, vol. 37, no. 8, pp. 1391–1393, 2012.
- [4] David Shrekenhamer, Claire M. Watts, and Willie J. Padilla, "Terahertz single pixel imaging with an optically controlled dynamic spatial light modulator," *Optics express*, vol. 21, no. 10, pp. 12507–12518, 2013.
- [5] Claire M. Watts, David Shrekenhamer, John Montoya, Guy Lipworth, John Hunt, Timothy Sleasman, Sanjay Krishna, David R. Smith, and Willie J. Padilla, "Terahertz compressive imaging with metamaterial spatial light modulators," *Nature Photonics*, vol. 8, no. 8, pp. 605–609, 2014.
- [6] Zhenwei Xie, Xinke Wang, Jiasheng Ye, Shengfei Feng, Wenfeng Sun, Tahsin Akalin, and Yan Zhang, "Spatial terahertz modulator," *Scientific Reports*, vol. 3, no. 1, pp. 97, 2013.
- [7] S. Augustin, J. Hieronymus, P. Jung, and H.-W. Hübers, "Compressed sensing in a fully non-mechanical 350 ghz imaging setting," *Journal of Infrared, Millimeter, and Terahertz Waves*, vol. 36, no. 5, pp. 496–512, 2015.
- [8] Rayko Ivanov Stantchev, Baoqing Sun, Sam M. Hornett, Peter A. Hobson, Graham M. Gibson, Miles J. Padgett, and Euan Hendry, "Noninvasive, near-field terahertz imaging of hidden objects using a single-pixel detector," *Science advances*, vol. 2, no. 6, pp. e1600190, 2016.
- [9] G. Kirchhoff, "Zur theorie der lichtstrahlen," *Annalen der Physik*, vol. 254, no. 4, pp. 663–695, 1883.
- [10] R. Kueng and P. Jung, "Robust Nonnegative Sparse Recovery and the Nullspace Property of 0/1 Measurements," *IEEE Trans. Inf. Theory*, vol. pp. no. 99, 2017.
- [11] D. Kim, S. Sra, and I. S. Dhillon, "A non-monotonic method for large-scale non-negative least squares," *Optimization Methods and Software (OMS)*, Jan. 2012.
- [12] Hendrik Dirks, "A flexible primal-dual toolbox," *ArXiv e-prints*, Mar. 2016.
- [13] Martin Slawski and Matthias Hein, "Non-negative least squares for high-dimensional linear models: Consistency and sparse recovery without regularization," *Electronic Journal of Statistics*, vol. 7, no. 1, pp. 3004–3056, 2013.